Meteorol Atmos Phys (2007)
DOI 10.1007/s00703-007-0271-6
Printed in The Netherlands

Meteorology and Atmospheric Physics

[1] Geophysical Institute and College of Natural Science and Mathematics, University of Alaska Fairbanks, Fairbanks, AK, USA
[2] School of Environmental Sciences, University of East Anglia, Norwich, UK

Use of atmospheric radiation measurement program data from Barrow, Alaska, for evaluation and development of snow-albedo parameterizations

N. Mölders[1], H. Luijting[2], K. Sassen[1]

With 8 Figures

Received 20 September 2006; Accepted 4 July 2007
Published online 10 October 2007

Summary

Snow albedo is determined from the ratio of out-going to incoming solar radiation using three years of broadband shortwave radiometer data obtained from the Barrow, Alaska, Atmospheric Radiation Measurement (ARM) site. These data are used for the evaluation of various types of snow-albedo parameterizations applied in numerical weather prediction or climate models. These snow-albedo parameterizations are based on environmental conditions (e.g., air or snow temperature), snow related characteristics (e.g., snow depth, snow age), or combinations of both. The ARM data proved to be well suited for snow-albedo evaluation purposes for a low-precipitation tundra environment. The evaluation confirms that snow-age dependent parameterizations of snow albedo work well during snowmelt, while parameterizations considering meteorological conditions often perform better during snow accumulation. Current difficulties in parameterizing snow albedo occur for long episodes of snow-event free conditions and episodes with a high frequency of snow events or strong snowfall.

In a further step, the first two years of the ARM albedo dataset is used to develop a snow-albedo parameterization, and the third year's data serves for its evaluation. This parameterization considers snow depth, wind speed, and air temperature which are found to be significant parameters for snow-albedo modeling under various conditions. Comparison of all evaluated snow-albedo parameterizations with this new parameterization shows improved snow-albedo prediction.

Correspondence: Nicole Mölders, Geophysical Institute and College of Natural Science and Mathematics, University of Alaska Fairbanks, 903 Koyukuk Drive, P.O. Box 757320, Fairbanks, AK 99775-7320, USA (E-mail: molders@gi.alaska.edu)

1. Introduction

Large parts of North America and Eurasia are seasonally snow-covered (e.g., Robinson et al. 1993). Thus, snow plays an important role in the surface energy budget in these regions (e.g., Abdalati and Steffen 1997; Cline 1997; Plüss and Ohmura 1997; Baker et al. 1999) because it changes the surface albedo from about 0.05 to 0.15 typical of dark soil, to about 0.95 or so for fresh snow (e.g., Oke 1978; Robinson et al. 1993; Boone and Etchevers 2001). The enlarged albedo of snow-covered surfaces will reflect more incoming shortwave radiation to space than snow-free surfaces do, thereby cooling the surface and atmosphere. The resulting relatively cooler conditions can lead to more snow refreshing the surface albedo and potentially increasing the snow coverage. Due to this positive snow-temperature-albedo feedback General Circulation Models (GCMs) and Numerical Weather

Prediction Models (NWPMs) require a good representation of snow albedo.

Snow albedo depends on precipitation history, snow depth, radiation, sun angle, wavelength, grain size and type, liquid water content of the snowpack, meteorological conditions, and air pollution effects (e.g., Warren and Wiscombe 1980; Wiscombe and Warren 1980; Brun et al. 1992; Essery and Etchevers 2004). In the presence of clouds, cloud properties alter snow albedo by changing the spectral distribution of the incoming radiation (Curry et al. 1993). Each snow event refreshes snow albedo. Since incoming radiation penetrates some depth into the snow, radiation still can be reflected from the surface underneath thin snowpacks (Wiscombe and Warren 1980). The absorption coefficient plays a major role for snow albedo. The solar zenith determines the angle of the radiation that reaches the snow surface and thereby snow albedo. Crystal size and type affect the reflection of light and at all wavelengths snow albedo decreases as the grain size increases and snow ages (Wiscombe and Warren 1980). Liquid water reduces snow albedo by increasing the grain-growth rate and effective grain size (O'Brien and Munis 1975). Thus, wet or refrozen snow is darker than fresh dry snow. Since air and snow-surface temperatures affect the melting of snow and freezing of water, these quantities also influence snow albedo. In summary, snow metamorphism alters snow albedo, as it modifies snow crystals, grain sizes, snow density and snow depth by wind break, phase transitions, meltwater percolation, compaction and settling. Aerosols deposited on or incorporated in the snow decrease reflectivity and albedo (Wiscombe and Warren 1980).

The Snow Models Intercomparison Project (SnowMIP; Essery and Yang 2001; Essery and Etchevers 2004; Etchevers et al. 2004) attempted to identify processes important for various applications (e.g., numerical weather prediction, climate simulations, snow-physics modeling). Due to the coarse grid resolution of NWPMs and GCMs, and because such models usually address questions where high-latitude processes are of less relevance, simulation of snow albedo is often over-simplified in their land surface models (LSMs). Snow-albedo parameterizations seldom distinguish between the calculation of snow albedo from direct and diffuse radiation in visible and near-infrared bands (Essery and Yang 2001), or consider radiative conditions (Etchevers et al. 2004).

The simplest representations of snow albedo use a fixed value. In the Semi-distributed Parameterization Scheme of the Orography-induced hydrology LSM, for instance, snow albedo is set equal to 0.75 when snow depth reaches a critical threshold (Shmakin 1998). Such simple changing of surface albedo values to values typical for snow, however, can lead to even opposite effects in simulated surface fluxes, soil- and near-surface temperatures than usually associated with a snow-cover (Fröhlich and Mölders 2002).

A second group of snow-albedo parameterizations relies on temperature conditions. The Best Approximation of Surface Exchange (BASE) scheme, for example, calculates a metamorphism factor based on the snow-temperature regime. Snow albedo will be 0.67 if the snow temperature is 0 °C and will increase to a maximum value of 0.85 as snow temperature reaches −10 °C (e.g., Desborough and Pitman 1998; Slater et al. 2001).

A third type of snow-albedo parameterization prognoses snow albedo depending on snow age (e.g., the Hydro-Thermodynamic Soil Vegetation Scheme (HTSVS); Kramm et al. 1996; Mölders et al. 2003).

Most snow-albedo parameterizations used in GCMs or NWPMs apply combinations of various environmental conditions and snow properties. The Geophysical Fluid Dynamics Laboratory LSM (Manabe 1969), for instance, prescribes a snow albedo according to surface temperature and snow depth; the Biosphere-Atmosphere Transfer Scheme (e.g., Yang et al. 1997) and Common Land Model (e.g. Zhou et al. 2003) consider snow age, solar zenith angle and the effect of dirt and soot to calculate snow albedo; and the Snow-Atmosphere-Soil Transfer (SAST) parameterization uses snow age, snow depth, cloud amount, and sun elevation angle (Sun et al. 1999).

Snow physics models (e.g., Brun et al. 1989, 1992; Jordan 1991; Durand et al. 1993; Flerchinger et al. 1996; Lehning et al. 1998) typically consider grain size and crystal structure to determine snow albedo. Models developed to directly predict snow albedo base on radiation-transport theory. They range from geometrical optics (e.g., Bohren and Barkstrom 1974), two-stream (e.g., Dunkle and Bevans 1956) to δ-

Eddington (e.g., Wiscombe and Warren 1980) methods. Since such sophisticated snow (albedo) models work on the small scale and since even homogenous snow layers have considerable horizontal variability (e.g., Brun et al. 1992), their approaches are not applicable in NWPMs or GCMs that operate at the mesoscale or global scale.

The simple parameterizations are directly calibrated with field data of one or more sites (cf. Mölders et al. 2003; Pedersen and Winther 2005). These simple parameterizations provide snow albedo as the ''outcome'' of given (meteorological) conditions rather than describing the actual physical processes. On the contrary, in sophisticated snow models, snow-albedo parameterization bases on albedo measurements and metamorphism laws derived from specific experiments in cold laboratory or field. In laboratory experiments, samples from the same snowfall are exposed to different possible environmental conditions for a defined time. Sub-samples taken at different depths from each snow sample at specified time intervals are characterized under the microscope to determine crystal type, growth rate and mean radius of curvature (e.g., Brun et al. 1992; Legagneux et al. 2004). Concurrent snow-albedo measurements permit deriving a relationship between snow albedo and crystal size, type and age of the snow surface (e.g., Wiscombe and Warren 1980). Other parameters determined are snow density and stratification (e.g., Dominé et al. 2002).

An intercomparison of seven GCM snow-albedo parameterizations and a multiple linear regression model and validation against data from eight sites showed that the prognostic parameterizations had a similar performance, as the temperature dependent parameterizations were similar to each other (Pedersen and Winther 2005). Temperature, snow depth, and positive degree day are significant (at the 95% confidence level) meteorological parameters for modeling snow albedo for most of these sites.

By using snow albedo and snow-surface temperature measurements the SnowMIP evaluated several snow models with respect to their simulation of the surface energy budget. For selected periods without precipitation this study showed that snow-albedo parameterizations based on snow age alone are accurate for melting periods, while surface-temperature based parameterizations are accurate for non-melting periods. In most cases, however, more complex parameterizations based on snow age and grain size are the most accurate (Etchevers et al. 2004).

In GCMs and NWPMs, often a grid cell is only partly snow-covered. Moreover, the snow albedo of an area strongly depends on fraction of melting snow, terrain elevation, steepness and orientation of slopes, and land cover (e.g., Roesch et al. 2001; Liston 2004; Essery et al. 2005). The presence of vegetation sticking out of snow cover decreases snow albedo by providing shadow, increasing the absorptance in the visible range and masking snow from exposure to the sun (e.g., Zhou et al. 2003). Masking of snow-covered ground by the canopy of coniferous forests, for instance, results in 60–75° N-area-averged albedo of 0.43 with locally even lower values (Robinson and Kukla 1985). GCMs and NWPMs without consideration of explicit vegetative masking for vegetation reaching out of the snowpack fail to capture the temperature-albedo feedback; thus, they may be cold-biased during spring when vegetative snow masking has its greatest effect on the surface energy budget north of 60° N (e.g., Tao et al. 1996). For these and other reasons various parameterizations to determine heterogeneity of precipitation and snow fraction have been developed (e.g., Leung and Ghan 1995; Roesch et al. 2001; Liston 2004). Some LSMs calculate snow-cover fraction as a function of snow-water equivalent (e.g., Ek et al. 2003), while others relate snow fraction to snow depth (e.g., Dai et al. 2001). Physically appropriate calculation of the energy fluxes of a partly snow-covered grid cell requires solving energy balances for the snow-covered and snow-free fraction separately (e.g., Liston 2004). Therefore, typically grid-cell ''total albedo'' is an area-weight of snow albedo and snow-free surface albedo that are calculated separately (e.g., Dai et al. 2003). Satellite data are best suitable for evaluation of snow-fraction parameterizations, regional and/or grid-cell averages of albedo because the satellite ''sees'' the vegetative masking effect (e.g., Robinson and Kuhkla 1985; Zhou et al. 2003). Comparison of seven modern snow-fraction parameterizations showed the same characteristics of a steep increase of snow fraction with snow depth, but differences in horizontal growth rate (e.g., Pedersen and Winther 2005). However, determining snow albedo correctly is an impor-

Fig. 1. Photograph of the upward and downward viewing radiometers used to determining the snow albedo at the North Slope Barrow, Alaska (USA), ARM site. Source: http://www.arm.gov/instruments/instrument.php?id = 15

tant pre-requisite for obtaining appropriate regional and/or grid-cell albedo averages.

The goal of our study is to use an extended radiometer dataset from the Atmospheric Radiation Measurement (ARM) program (Stokes and Schwartz 1994) available for the evaluation and development of snow-albedo parameterizations for low-precipitation tundra environments. The remote location of the ARM site at Barrow, Alaska (Fig. 1), guarantees that snow is relatively pristine, i.e. the impact of air pollutants on snow albedo is marginal. Most of the few Alaska pollutants stem from far-range transport of constituents emitted in Eurasia (e.g., Shaw 1991; Cahill 2003). Moreover, the flat treeless terrain has a closed snow cover until snowmelt. Out of the variety of snow-albedo parameterizations used in NWPMs or GCMs we chose representative examples of common approaches. As a courtesy to the reader we also indicate which other LSMs apply these or similar parameterizations, and compare our results to other evaluation studies.

2. Experimental design

2.1 ARM radiometric data

To determine snow albedo we use data of incoming and outgoing shortwave radiation measured in the ARM site (Ellingson et al. 1999) at Barrow (71°18′N, 156°47′W) from 2001 to 2003. Barrow is located on the North Slope at the northernmost point in the United States, 1080 km north of the Arctic Circle. Barrow has an Arctic climate (About $1.74 \times 10^6\,\mathrm{km}^2$ of the Northern Hemispheric continents have Arctic climate) and is located in a tundra landscape. Note that tundra covers about $7.34 \times 10^6\,\mathrm{km}^2$ of the global landmass (e.g., Matthews 1983). Temperatures stay below freezing point for most of the year with February being the coldest and July being the warmest month. Spring starts in May, and summer ends in September. At Barrow, the sun remains above the horizon from May 10 to August 2, and below the horizon from November 18 to January 24 (Alaska Climate Research Center 2004). During polar night diffuse radiation is negligibly small (e.g., Curry et al. 1996).

Down-welling and upwelling shortwave radiation is measured at 1-min intervals by an unshaded pyranometer with a hemispheric field of view and an inverted Eppley Laboratory Inc., Precision Spectral Pyranometer (PSP). The pyranometer measures global hemispheric irradiance between 0.3 and 3 μm. The PSP is a World Meteorological Organization first class radiometer and provides continuous measurements of broadband shortwave (solar) irradiances for the upwelling component. This instrument's precision ground and polished hemispheres of clear WG295 Schott optical glass are uniformly transparent between 0.285 and 2.8 μm. This instrument's response time, sensitivity, and uncertainty are 1-s, $\sim 9\,\mu\mathrm{V}/\mathrm{W\,m}^{-2}$, and $\pm 3\%$ or $10\,\mathrm{W\,m}^{-2}$, respectively. Once a day Monday through Friday, the instruments are cleaned to remove water-vapor deposits, frost and snow.

There is typically enough sunlight to obtain values of the incoming and outgoing shortwave radiation suitable for snow-albedo calculation for about four months per year when we discard all data with less than $20\,\mathrm{W\,m}^{-2}$. January does not have enough sunlight for shortwave radiation measurements. The snowpack has usually melted

by mid May. Fall gives less data than spring because of the relatively late onset of snow and the decrease in daylight. For all remaining data (February to about mid-May, October to early November) we determine the snow albedo α from the ratio of outgoing $R_s^{\uparrow}$ to incoming shortwave radiation, $R_s^{\downarrow}$ by

$$\alpha = \frac{R_s^{\uparrow}}{R_s^{\downarrow}} \tag{1}$$

Any measurements are generally burdened with ''errors'' arising from natural (random) variability as expressed by the variance or standard deviation (e.g., Kreyszig 1970; Meyer 1975). In this case, $R_s^{\uparrow}$ and $R_s^{\downarrow}$ have the standard deviations (statistical uncertainty) $\sigma_{R_s^{\uparrow}}$ and $\sigma_{R_s^{\downarrow}}$, respectively. Consequently, any quantity calculated with these values is ''error''-burdened. The standard deviation of the calculated snow albedo can be determined by applying Gaussian error propagation principles (e.g., Kreyszig 1970; Meyer 1975; Mölders et al. 2005). Thus, snow-albedo standard deviation

$$\begin{aligned}\sigma_\alpha &= \pm\sqrt{\sigma^2_{R_s^{\uparrow}}\left(\frac{\partial\alpha}{\partial R_s^{\uparrow}}\right)^2 + \sigma^2_{R_s^{\downarrow}}\left(\frac{\partial\alpha}{\partial R_s^{\downarrow}}\right)^2} \\ &= \pm\sqrt{\sigma^2_{R_s^{\uparrow}}\left(\frac{1}{R_s^{\downarrow}}\right)^2 + \sigma^2_{R_s^{\downarrow}}\left(\frac{R_s^{\uparrow}}{(R_s^{\downarrow})^2}\right)^2}\end{aligned} \tag{2}$$

and relative error $\varepsilon = \frac{\sigma_\alpha}{\alpha}\,100\%$ vary from 0.026 to 0.329 and 3.7 to 57.6%, respectively (Fig. 2). Standard deviation decreases with increasing incoming shortwave radiation; i.e. albedo values are more accurate late in spring, early in fall and around local noon than early in the morning, early in spring or late in fall. The relative error nonlinearly decreases with increasing outgoing solar radiation (Fig. 2).

2.2 Meteorological data

The meteorological station at the ARM site is equipped with conventional Vaisäla in situ sensors. We use 2-min vector-averaged wind speeds recorded at 2-m height. The accuracy amounts to $\pm 0.17\,\mathrm{m/s}$ between 0.4 and 75 m/s.

The cumulative snow is employed to determine snow age, i.e. the time since the last snowfall. If the cumulative snow ($\Delta h_s = \rho_w \Delta h_w / \rho_s$ where ρ_w and ρ_s are the density of water and snow and Δh_w is the change in water equivalent) increases between any 2 time steps, this change, Δh_s, is counted as a snow event and the snow age is reset to zero. Snow depth is not directly measured within the ARM program at Barrow, so we use the data measured at the nearby (200 m) National Oceanic and Atmospheric Administration Climate Monitoring and Diagnostics Laboratory (CMDL). These measurements are taken at three places and averaged to the full inch because of the often windy condition (Fathauer 2006, pers. communication). The ARM and CMDL sites are surrounded by open fairly flat and sodden tundra, i.e. snowdrift conditions are comparable. Because of snowdrift snow depth often

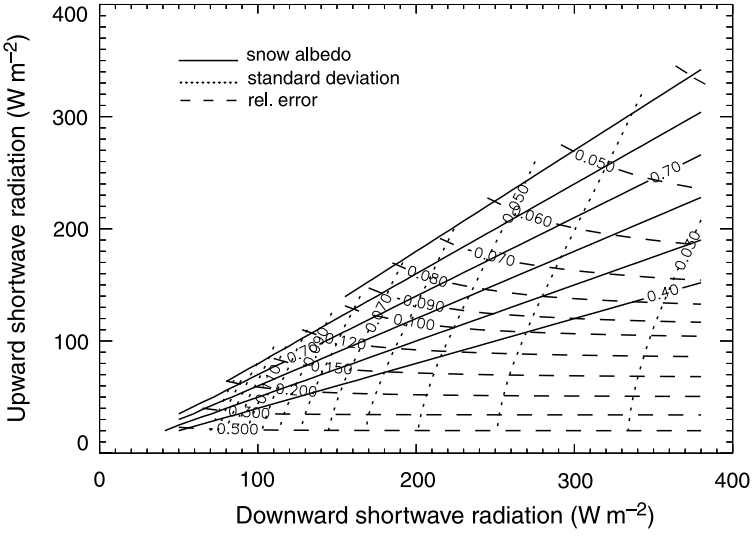

Fig. 2. Standard deviation and relative error of snow albedo (due to uncertainty in upward and downward shortwave radiation measurements) in dependence of upward and downward shortwave radiation for snow albedo values from 0.4 (dirty old snow) to 0.97 (Antarctica dry fine-grain snow average over five days (Liljequist 1956)). Note that contour lines of relative error (values between 0 and 1) have non-equal spacing. Note that these data do not represent the standard deviation over the day or season

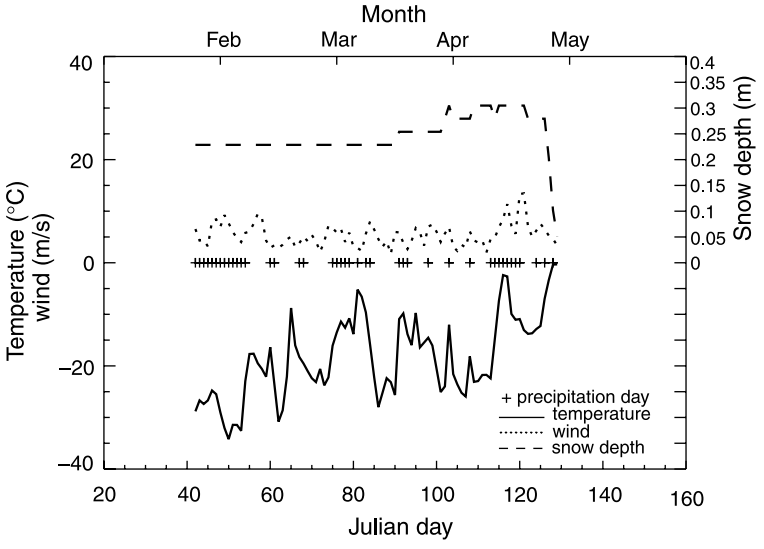

Fig. 3. Daily mean values of air temperature, snow depth, and wind speed at Barrow in 2002. Note that there is no data on cumulative snow available before Julian day 53, and between Julian days 75 and 79

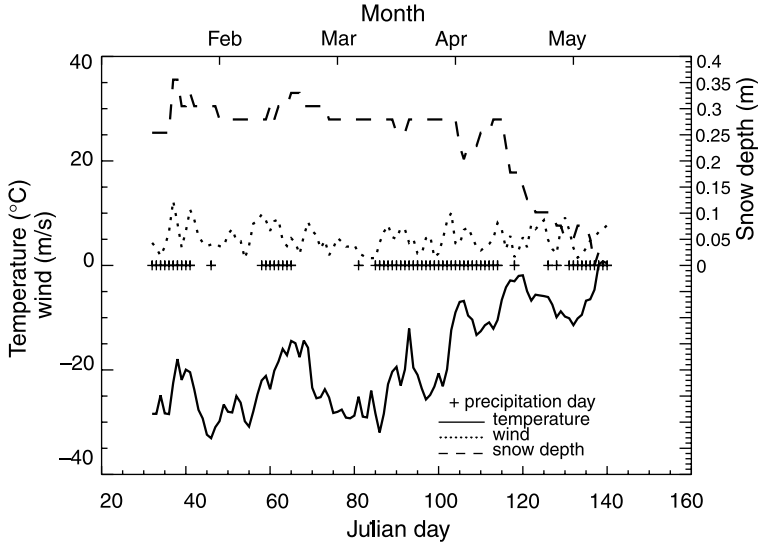

Fig. 4. Like Fig. 3, but for 2003. Note that there is no data on cumulative snow available between Julian days 85 and 111

does not increase after snowfall (Figs. 3 and 4). Note that at Barrow, trace precipitation occurs with high frequency and varies spatially (Yang and Woo 1999; Sugiura and Yang 2003), and measurements underestimate snowfall by up to 30% (Dingman 1994) at the wind speeds typical for Barrow. Because wind can suspend snow crystals and deposit them elsewhere (e.g., Liston and Sturm 1995), there is some uncertainty in snow depth and age.

We also use the CMDL air-temperature measurements since this is the more complete dataset. Missing data are replaced by data from ARM if possible. Temperature is measured every minute at 2-m height with a precision of 1 K.

3. Snow-albedo parameterization evaluation

Since a snow-albedo parameterization using a fixed value will only occasionally provide the right value by coincidence, we do not consider these parameterizations in our evaluation. For simplicity, in the following the snow-albedo parameterizations examined in this study as their results are addressed with the name of the model they are used in.

Since snow depth was measured every 24 h, daily values are the highest resolution possible for parameterizations using this quantity. Thus, we averaged the meteorological data to daily values. The albedo is determined every minute

using Eq. (1), then averaged over the hours where solar radiation exceeds $20\,\mathrm{W\,m^{-2}}$. Parameterizations not using snow depths are also run with the high resolution data. The daily average albedo values obtained this way marginally differ from the ones obtained when forcing the parameterizations with daily averages. For the plots, evaluation and the related statistics, daily averages are used for all parameterizations to keep the comparison fair.

The following evaluations are performed using observed meteorological forcing (e.g., Figs. 3 and 4). In GCMs or NWPMs, however, predicted winds and air temperatures are volume averages representative for a grid cell of several kilometers and meters in the horizontal and vertical direction; precipitation, radiation fluxes and snow depth are area averages (e.g., Jacobson 1999; Friedrich and Mölders 2000; Pielke 2002). In nature, conditions may vary appreciably in complex terrain, where channeling effects may strongly modify wind speed (e.g., Leung and Ghan 1995); snowdrift, slopes and their exposition may affect snow depth and distribution (e.g., Liston 2004). To account for these effects, some NWPMs and GCMs consider subgrid-scale variability of precipitation, snow depth, wind, temperature, and/or albedo (e.g., Seth et al. 1994; Leung and Ghan 1995; Mölders et al. 1996; Tetzlaff et al. 2002; Liston 2004). However, even in these parameterizations the respective quantities represent a large volume or area. Thus, one has to expect that discrepancies in predicted area snow albedo (even if the entire grid cell is snow-covered in nature and the model world) will result from using simulated forcing. Furthermore, discrepancies between simulated and observed snow albedo will be larger than those presented here if the snow-albedo parameterizations are driven with predicted forcing. Any forecast errors, namely, will propagate into errors of the calculated snow albedo according to Gaussian error propagation (cf. Kreyszig 1970; Meyer 1975; Mölders et al. 2005).

3.1 Temperature-dependent albedo

The snow albedo parameterization of the **E**uropean **C**enter for **M**edium-range Weather Forecast (ECMWF) model with the modification made at the Max Planck Institute **HAM**burg (ECHAM) depends solely on snow-surface temperature, T_{sf} (Roeckner et al. 1996; Loth and Graf 1998)

$$\alpha = \begin{cases} 0.8 - 0.4\dfrac{T_{\mathrm{sf}} - T_{\mathrm{min}}}{T_{\mathrm{m}} - T_{\mathrm{min}}} & T_{\mathrm{sf}} > -10\,^{\circ}\mathrm{C} \\ 0.9 & T_{\mathrm{sf}} \leq -10\,^{\circ}\mathrm{C} \end{cases}. \tag{3}$$

Here $T_{\mathrm{min}} = -10\,^{\circ}\mathrm{C}$ and $T_{\mathrm{m}} = 0.01\,^{\circ}\mathrm{C}$. This formulation leads to discontinuous behavior around $-10\,^{\circ}\mathrm{C}$. Since snow-surface temperature was not measured at Barrow, we use air temperature instead and limit its upper value to the freezing point (temperature of an isothermal melting snowpack). According to Eq. (3) minimum snow albedo is 0.4. This value was reduced to 0.3 for ECHAM5 (Roesch and Roeckner 2006).

Other examples for temperature dependent snow-albedo parameterizations are the BASE, HIRHAM (Dethloff et al. 1996), UK Meteorological Office (UKMO) model (Essery et al. 1999), and ECHAM5 (Roeckner et al. 2003).

3.2 Snow age

Most snow-albedo parameterizations that rely on snow age distinguish between air temperatures T_{R} below and above the freezing point T_0 by different functions for these two regimes. Herein, snow age is defined as the time passed since the last snowfall. The parameterization of HTSVS was derived from data published by the U.S. Corps of Engineers (1950, as cited by Dingman 1994) by (Mölders et al. 2003)

$$\alpha = \begin{cases} 0.35 + 0.18\exp\left(\dfrac{-t_{\mathrm{snow}}}{114048}\right) \\ \quad +0.31\exp\left(\dfrac{-t_{\mathrm{snow}}}{954720}\right), & \text{for } T_{\mathrm{R}} > T_0\,, \\ 0.61 + 0.23\exp\left(\dfrac{-t_{\mathrm{snow}}}{469411}\right), & \text{for } T_{\mathrm{R}} \leq T_0 \end{cases} \tag{4}$$

where t_{snow} (s) is snow age. Like in many other LSMs (e.g., Verseghy 1991; Loth and Graf 1998; Bonan et al. 2002) a minimum snow depth (1 mm) is assumed. Thus, for the change from snow-free to snow-covered conditions, the snowpack must exceed this threshold for snow albedo to be calculated. If the snowpack exceeds already this value, snowfall must exceed 0.1 mm water equivalent for the snow age to be reset to zero.

In the Interaction between Soil, Biosphere and Atmosphere (ISBA) parameterization, snow albedo is parameterized in accord with Verseghy (1991) and Baker et al. (1990) for the melting period and sub-freezing days, respectively (e.g., Douville et al. 1995; Boone and Etchevers 2001; Boone 2002)

$$\alpha_n = \begin{cases} \alpha_{n-1} - 0.008\dfrac{\Delta t}{86400} & T_{\mathrm{sf}} < T_0 \\ (\alpha_{n-1} - \alpha_{\min})\exp\left(-0.24\dfrac{\Delta t}{86400}\right) + \alpha_{\min} & T_{\mathrm{sf}} = T_0 \end{cases}, \tag{5}$$

where $\alpha_{\min} = 0.5$ is the minimum albedo, Δt (s) is the model time step, T_{sf} is surface temperature, T_0 is the freezing point. Furthermore, α_n and α_{n-1} denote the albedo of the current and previous time step, respectively. A snowfall of at least one centimeter water equivalent refreshes the snow albedo back to its maximum value of 0.85.

The snow model of the Instituto Nacional de Meteorologia (Fernandez 1998) uses the same parameterization as ISBA. Other LSMs relying on snow age for snow-albedo parameterization are the Goddard Institute for Space Studies' model (Hansen et al. 1983), Tohoku snow cover model I (Kondo and Yamazaki 1990), Distributed Hydrology Soil Vegetation Model (Wigmosta et al. 1994), Biosphere-Atmosphere Interaction Model (Mabuchi et al. 1997), and Tohoku snow cover model with multi-layers (Yamazaki 1998).

Note that parameterizations wherein snow albedo depends on the snow albedo of the previous time step are called prognostic. From a computational view there is no difference between expressing the snow-age dependence by the time after the last snowfall, t_{snow}, or the albedo of the previous time step, α_{n-1}. However, errors may propagate for the latter procedure. Other LSMs using a prognostic snow-albedo parameterization are CLASS, SAST and ECMWF model (cf. Pedersen and Winther 2005).

3.3 Combination of environmental conditions and snow properties

In the SAST parameterization, snow albedo α_n at time n is a function of temperature, T_{R}, snow depth, h_{s}, snow albedo of the previous time step, α_{n-1}, and snow age expressed by the model time step, $\Delta\tau(d)$. The parameterization is based on Gray and Ladine (1987) for shallow snow, and Verseghy (1991) for deep snow (Sun et al. 1999)

$$\alpha_{\mathrm{n}} = \begin{cases} \alpha_{n-1} - 0.006\Delta\tau & T_{\mathrm{R}} \le T_0 \\ 0.5 + (\alpha_{n-1} - 0.5)\exp(-0.24\Delta\tau) & T_{\mathrm{R}} > T_0 \wedge h_{\mathrm{s}} > 0.25\,\mathrm{m} \\ \alpha_{n-1} - 0.071\Delta\tau & T_{\mathrm{R}} > T_0 \wedge h_{\mathrm{s}} \le 0.25\,\mathrm{m} \end{cases}. \tag{6}$$

Every centimeter of new snow increases the snow albedo by 0.1. The maximum albedo for fresh snow is 0.92. Other examples for snow-albedo parameterizations considering these quantities are the Goddard Space Flight Center GCM (Manabe 1969), the Regional Atmospheric Modeling System (Strack et al. 2004), and the Arctic Regional Climate System Model (ARCSM; e.g., Lynch et al. 1995).

4. Results

We evaluate the performance of the parameterizations by comparison of simulated and measured snow albedo. To elaborate the differences in overall performance and potential reasons therefore, we calculate various skill cores (e.g., Anthes et al. 1989). The BIAS assesses systematic errors from consistent misrepresentation of geometrical, physical, or numerical factors; the Standard Deviation of Error (SDE) represents random errors caused by uncertainty in initial conditions or observations. The Root Mean Square Error (RMSE) identifies the offset between simulation and observation. Together with the correlation coefficient the goodness of fit can be evaluated (Fig. 5). Results of out-layer tests made for each parameterization will be discussed, if simulated and observed values differ more than a factor of 2. A student t-test is performed to examine whether simulated and observed mean snow-albedo distributions are the same (null hypothesis) or significantly different (at the 95% confidence level). Note that the mean snow albedo measured for Barrow is 0.81 for the data used in this study with an average snow albedo of 0.79 in 2001 and 2002 and 0.82 in 2003, respectively.

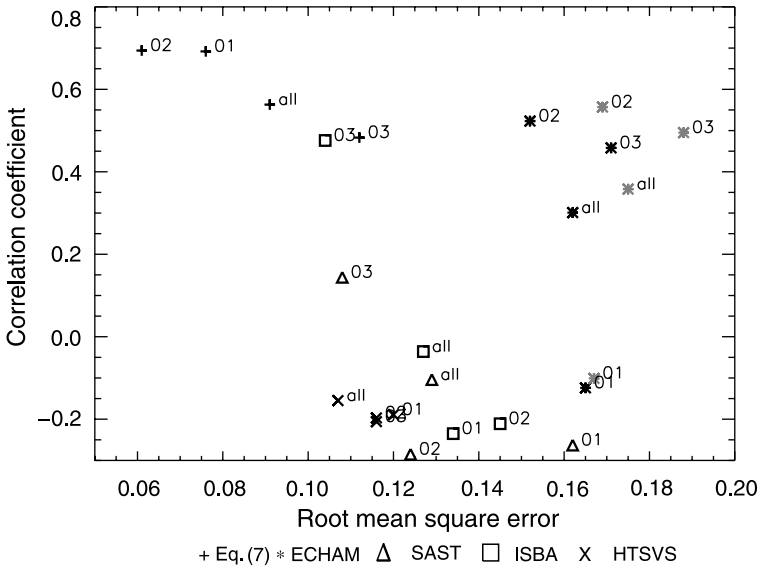

Fig. 5. Scatter plot of RMSE against correlation of simulated and observed snow albedo for the various parameterizations and years. A good parameterization has a small RMSE and high correlation coefficient. The labels all, 01, 02, and 03 stand for 2001 to 2003, 2001, 2002, and 2003, respectively

4.1 Temperature-dependent albedo

At Barrow like in many other high-latitude locations air temperatures stay below −10 °C for prolonged periods during the cold season (Figs. 3 and 4). Thus, ECHAM's snow-albedo parameterization overestimates the snow albedo regularly and is not able to capture the temporal pattern (Fig. 6a). Maximum albedo seems too high. In March and May 2002, for instance, simulated and observed snow albedo disagree more than a factor of 2 for 2 and 5% of the time. In 2001 and 2003, such disagreement occurs about 1 and 2% of the time. During episodes with temperatures warmer than −10 °C the parameterization performs acceptably (e.g., Figs. 3 and 6a; Julian days 115–118). Then, however, the SDE increases because the inclusion of temperature contributes observational uncertainty measured by the SDE, while below this threshold, observational errors occur only for snow albedo (Table 1). In episodes without snow event, ECHAM overestimates the temporal decrease (Fig. 6a). However, once a strong snowfall occurs during relatively warm conditions, it captures snow albedo well (e.g., Fig. 6a, in mid-May). Like found for other temperature dependent parameterizations (UKMO, ECHAM5; cf. Pedersen and Winther 2005; HIRHAM; cf. Liu et al. 2007) ECHAM's snow albedo decreases too early and too fast during snowmelt. The fixed minimum albedo seems unrealistically low. Pederson and Winther (2005) found similar results for ECHAM5. A sensitivity study performed using the new minimum albedo of ECHAM5 shows similar shortcomings than ECHAM (Figs. 6a and 7a). These shortcomings result into insignificant correlation of simulated and observed snow albedo for 2001 and 2002 and overall (Fig. 5) and even a negative correlation for some months. The RMSEs obtained for Barrow with ECHAM5 are slightly higher than the mean RMSE of the eight sites examined by Pedersen and Winther (2005), but are less than their maximum RMSE. Allowing snow-surface temperature to be above the freezing point (dirty snow) slightly improves the correlation, but increases the RMSE.

4.2 Snow age

Both parameterizations are very sensitive to the snowfall threshold for reset of snow age. The sensitivity to uncertainty in cumulative snowfall measurements and threshold values was also reported by Pedersen and Winther (2005) for other snow-albedo parameterizations.

The HTSVS snow-albedo parameterization underestimates snow albedo especially in March 2002 and 2003, and April 2002 (Figs. 6b and 7b). The rate of decrease in snow albedo is greater in the simulation than in nature. This leads to relatively high RMSEs in February, March, and October. Correlation between simulated and observed snow albedo is often negative in February and March, and results in an overall negative correlation for 2001 and 2002 and the three years (Fig. 5). However, the HTSVS snow-albedo

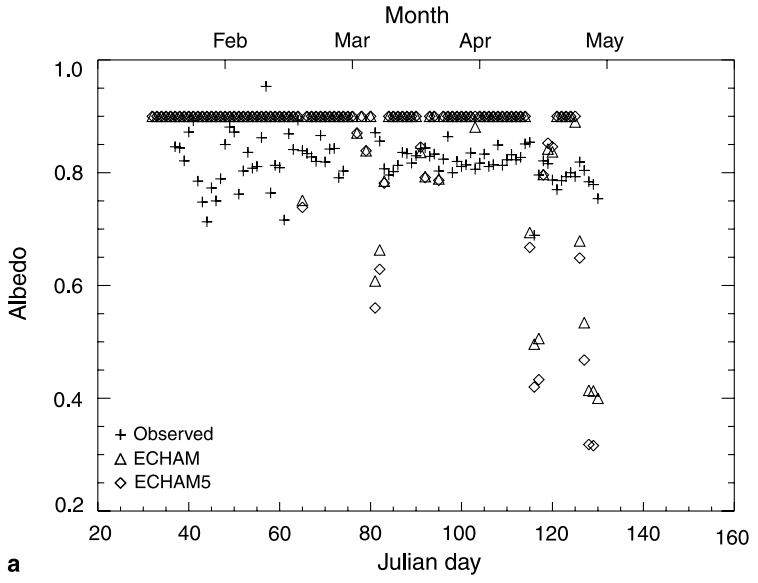

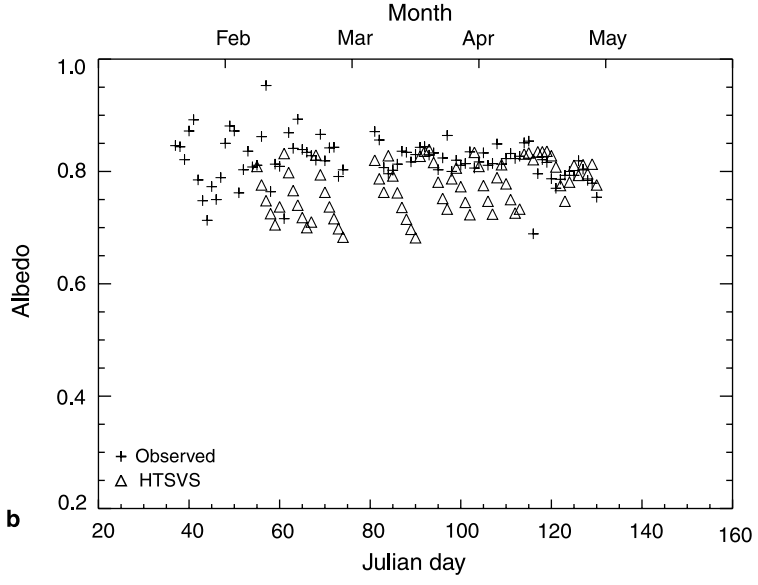

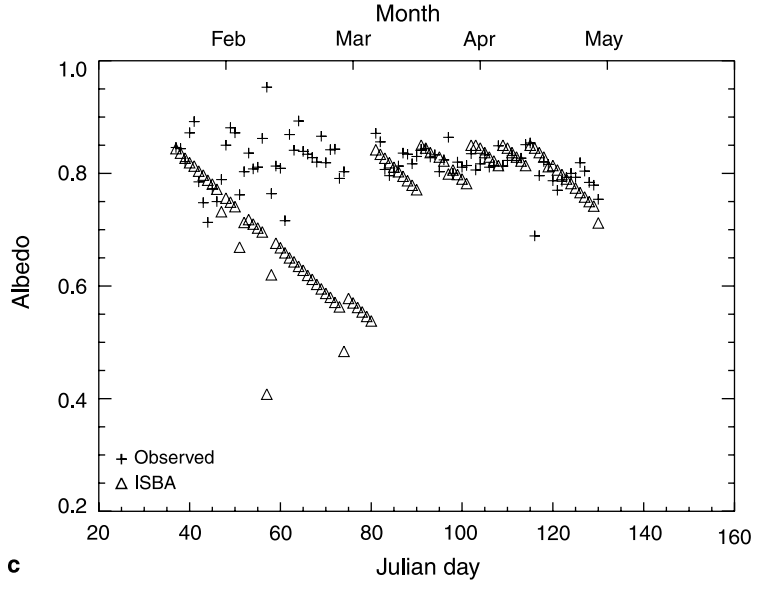

Fig. 6. Daily mean values of snow albedo as simulated by the snow-albedo parameterizations of (**a**) ECHAM, (**b**) HTSVS, (**c**) ISBA, (**d**) SAST, and (**e**) the new parameterization compared to the daily mean snow albedo at the ARM site for February to May 2002. Results for October and November are not shown. Note that there is no data on cumulative snow available before Julian day 53, and between Julian days 75 and 79 so that snow albedo cannot be determined for HTSVS

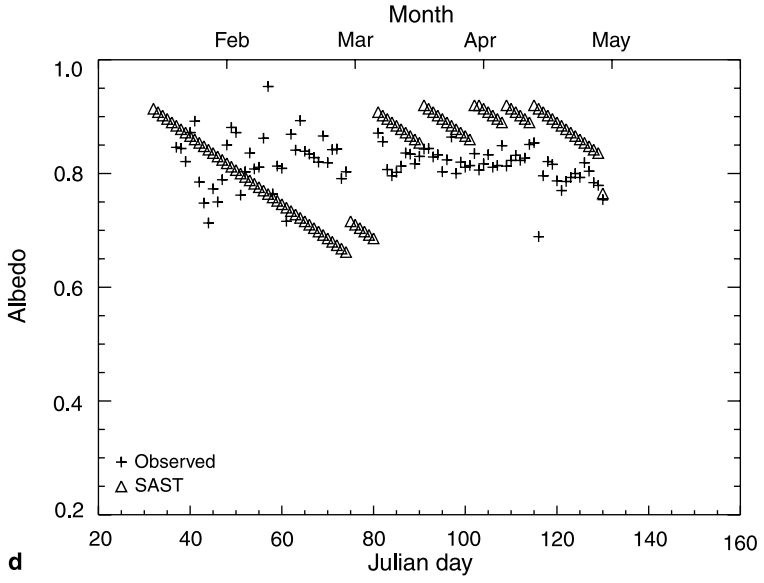

d

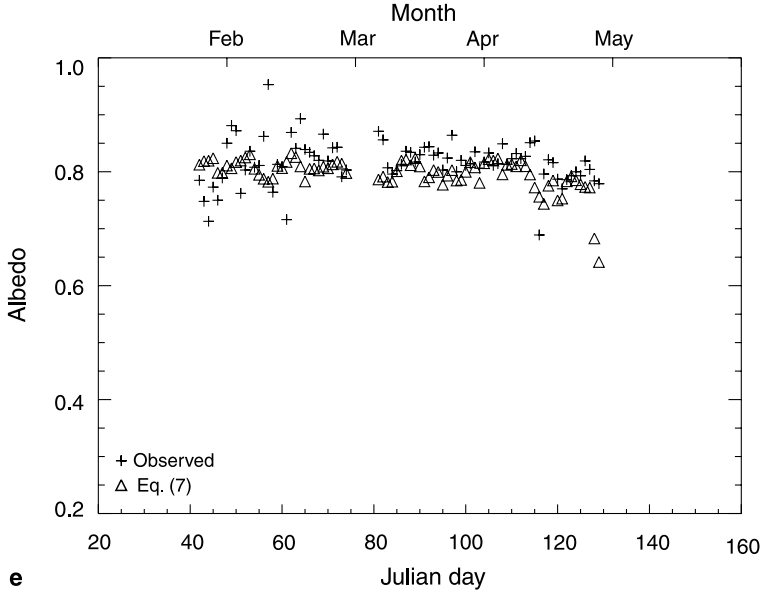

e

Fig. 6 (*Continued*)

parameterization performs well when temperatures increase in the melting season (e.g., Fig. 6b; Julian day 115 onwards). During snowmelt, RMSEs, SDEs, and BIAS are about half of those of the other months, and the correlation coefficient increases to 0.621. The overall BIAS is very small in 2001 and 2002, but about an order of magnitude larger in 2003 (Table 1). The choice of the maximum values plays a role. Average observed snow albedo was higher in 2003 than 2001 and 2002, making a systematic underestimation of snow albedo more likely as reflected by the increased BIAS. By increasing the maximum value to 0.89 the 2003 BIAS decreases, and the 2001 and 2002 BIAS increase and change sign. Some discrepancies result from the data used for developing the snow-albedo parameterization of HTSVS. Unlike in the continental US, where the data used in the parameterization development were collected, in Alaska, there is less industry and pollution. Thus, at Barrow, aerosols deposit at a comparatively lower rate on the snow; this may explain the overestimation of the decrease in albedo. In summary, this parameterization works better at relatively warmer conditions than extremely cold ones.

In contrast to HTSVS, ISBA relies on the previous snow albedo for determination of the next value rather than the time past since the last snowfall. In 2002 and 2003 and overall, snow

Table 1. BIAS, SDE, and mean for snow albedo as obtained for ECHAM, HTSVS, ISBA, SAST and the new parameterization. Mean snow albedo amounts 0.79, 0.79, 0.82, and 0.81 for 2001, 2002, 2003, and 2001–2003, respectively. Bold numbers indicate that the simulated and observed means of snow albedo differ significantly at the 95% confidence level

	ECHAM	HTSVS	ISBA	SAST	New parameterization
2001					
SDE	0.153	0.120	0.132	0.127	0.075
BIAS	−0.061	0.006	−0.021	−0.099	0.012
Mean	**0.851**	0.801	**0.811**	**0.890**	0.769
2002					
SDE	0.151	0.088	0.143	0.110	0.060
BIAS	0.020	0.009	0.029	−0.058	0.009
Mean	**0.775**	0.783	**0.766**	**0.853**	0.775
2003					
SDE	0.161	0.089	0.088	0.099	0.092
BIAS	0.058	0.080	0.056	−0.043	0.064
Mean	0.764	0.754	**0.782**	**0.866**	0.760
2001–2003					
SDE	0.162	0.103	0.124	0.112	0.08
BIAS	0.015	0.031	0.027	−0.062	0.032
Mean	**0.790**	0.778	**0.777**	**0.867**	0.766

albedo simulated by ISBA only agrees with the observation within a factor of 2 in about 98, 99 and 99% of the cases. ISBA performs well as long as there are numerous snow events so that the snow albedo is reset to the maximum value (e.g., Fig. 6c, Julian days 91–120). The parameterization underestimates the snow albedo in months with few snow events (e.g., Fig. 6c, Julian days 83–90). These findings well agree with Pedersen and Winther's (2005) results found with ISBA for Ny-Ålesund another low precipitation site. This shortcoming often leads to negative correlations in February and March that then result in a negative correlation over the season (Fig. 5). Like HTSVS, ISBA performs best during the melting season (e.g., Fig. 6c), but has greater RMSE than HTSVS. ISBA's overall RMSE of about 0.13 obtained for Barrow (Fig. 5) well fits into the range (0.08–0.21) found for the eight sites evaluated by Pedersen and Winther (2005), but the overall correlation is comparatively weaker for Barrow. During snowmelt, however, correlation amounts 0.664.

For all years simulated and observed mean snow albedo differ significantly. The 2003 RMSE is smaller and the correlation is higher (Fig. 5), but the BIAS is larger than for the other years (Table 1). Overall there is more snow in 2003. Obviously, the threshold and increment for refreshing snow albedo cause systematic errors.

The different BIAS behavior of ISBA and HTSVS can be explained by the treatment of snow age: In HTSVS, each snow event greater than 1 mm refreshes snow albedo to 0.84, while in ISAB each centimeter of snow increase albedo by 0.1 until 0.92 is reached (e.g., Figs. 6b, c, and 7b, c). Despite this advantage of HTSVS, we conclude that both parameterizations have difficulties with low precipitation conditions and perform best in the melting season. The fact that the snow-age dependent parameterizations perform best in the melting season well agrees with findings from SnowMIP (e.g., Etchevers et al. 2004).

4.3 Combination of environmental conditions and snow properties

At Barrow, seldom temperatures are above freezing and snow depth exceeds 0.25 m at the same time. Thus, for Arctic conditions SAST works like an age dependent only parameterization most of the time (cf. Eq. (6)). Simulated snow albedo gradually decreases until the next snowfall, i.e.,

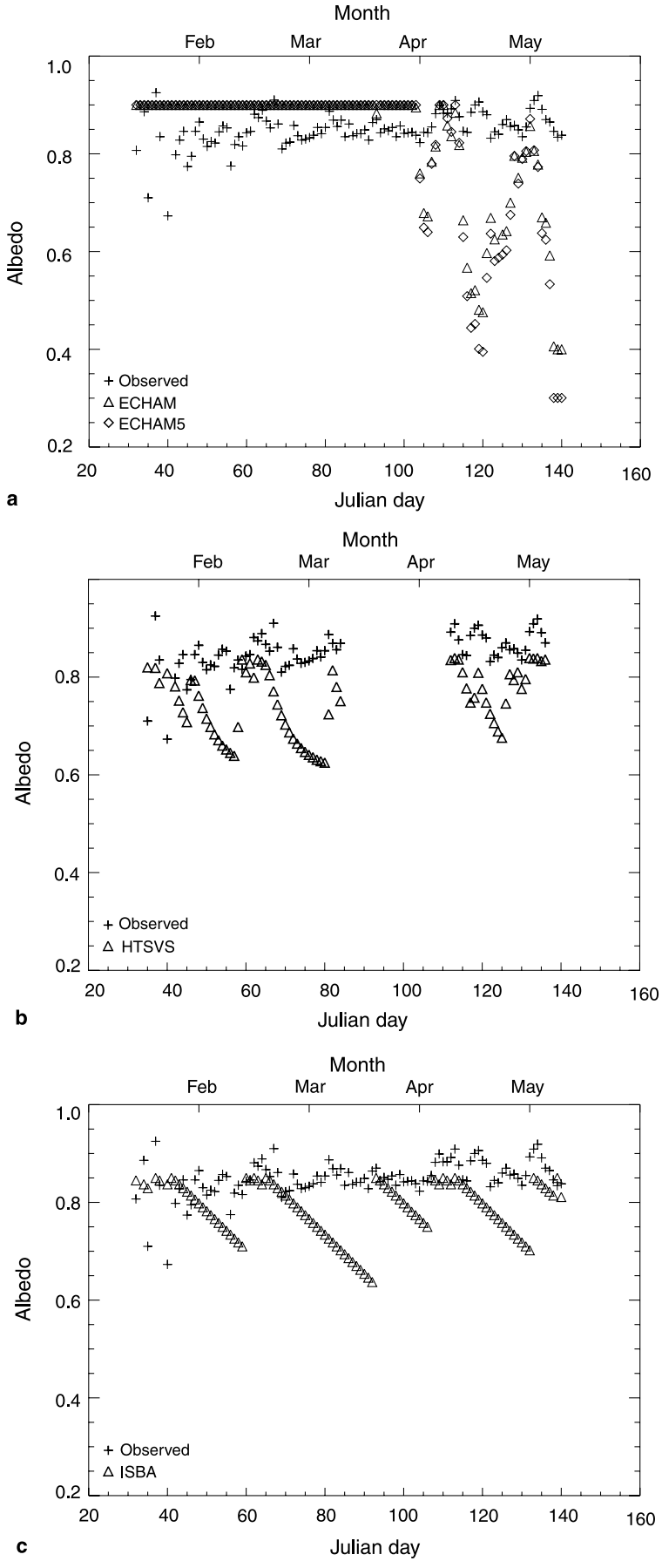

Fig. 7. Like Fig. 6, but for 2003. Note that there is no data on cumulative snow available between Julian days 85 and 111 so that snow albedo cannot be determined for HTSVS

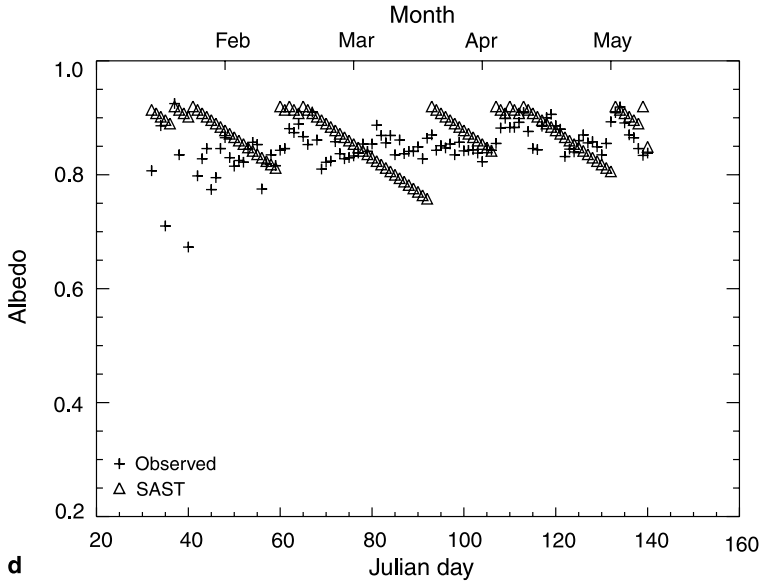

d

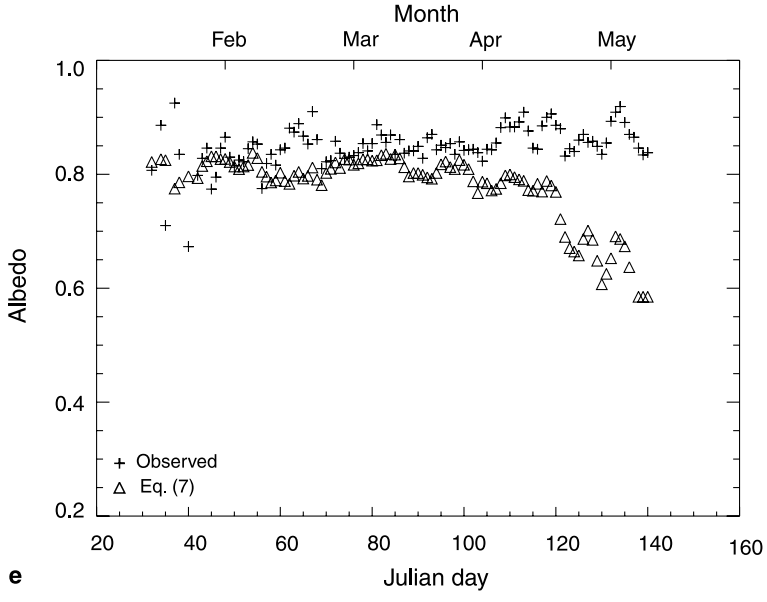

e

Fig. 7 (*Continued*)

like HTSVS and ISBA, SAST misses the temporal pattern between snow events (e.g., Fig. 6d). Frequently, the amount of new snow is large enough to refresh the snow albedo to the maximum value of 0.92 (e.g., Fig. 6d, Julian days 91, 102, 103, 109, and 114). This value seems to be too high, for which snow albedo is overestimated most of the time (e.g., Fig. 6d). Note that Liu et al. (2007) also found overestimation of snow albedo for ARCSM that considers surface temperature and snow depth. Like for ISBA, any snowfall less than one centimeter will not refresh snow albedo in SAST. In March, differences between simulated and observed values are often larger than ± 0.2 and SDE exceed those of the other months. Here uncertainty in trace precipitation and cumulative snow play a role. During long periods without snowfall (e.g., Figs. 3, 4, 6d, 7d; Julian days 67–74, 83–90 in 2002, 63–80 in 2003), snow albedo is underestimated because the simulated decrease is too rapid. The often relatively low RMSEs (Fig. 5) are more due to the closeness of simulated albedo to the magnitude of the observed value than due to capturing the temporal pattern. Often, SAST simulates a decrease when snow albedo increases in nature (e.g., Fig. 6d, Julian days 43–49, 118–125). Consequently, correlations are negative for some months and overall insignificant. For all years, there is a negative BIAS (Table 1).

5. Development of a snow-albedo parameterization

To develop a parameterization of snow albedo, we use the temperature, wind speed, snow depth and snow-age data, quantities that are usually simulated or diagnosed by GCMs and NWPMs. We split the ARM dataset into two parts using the 2001 and 2002 data for the snow-albedo parameterization development, and the 2003 data for evaluation. The suitability of ARM data for the development of snow-albedo parameterizations is judged based on the 2003 data on the improvement gained by the new parameterization as compared to those evaluated before. Since snow depth and precipitation data only exist on a daily basis, we use daily averages in all analysis including this quantity.

5.1 Influence of meteorological conditions on snow albedo

The hypothesis that a meteorological parameter contributes to modeling snow albedo is tested versus that it does not using a 95% confidence level. Temperature and wind are found as significant parameters at the ARM site for 2003, and snow depth for 2001 and 2002. Note that Pedersen and Winther (2005) who applied such a test for data from Svalbard, Cole de Porte, Ny-Ålesund, and six sites in the former Soviet Union, found temperature, snow depth, and positive degree-day as the significant parameters except for one site where wind and temperature are the significant parameters. At Barrow, temperatures remain below zero on 94% of the days for which snow-albedo data are available. Therefore positive degree-day is an insignificant parameter.

The correlation between the snow albedo and temperature, snow depth, wind speed and snow age is analyzed using daily mean values from 206 days in 2001 and 2002 (e.g., Fig. 8). First we calculate the correlation between albedo and each variable separately using the Pearson correlation coefficient of two vectors.

Snow albedo and air temperature correlate weakly ($r = -0.268$), indicating a decrease of snow albedo as temperature increases. This result agrees with the expectations that snow albedo decreases as temperature and hence effective grain size, liquid water content and/or growth rate increase.

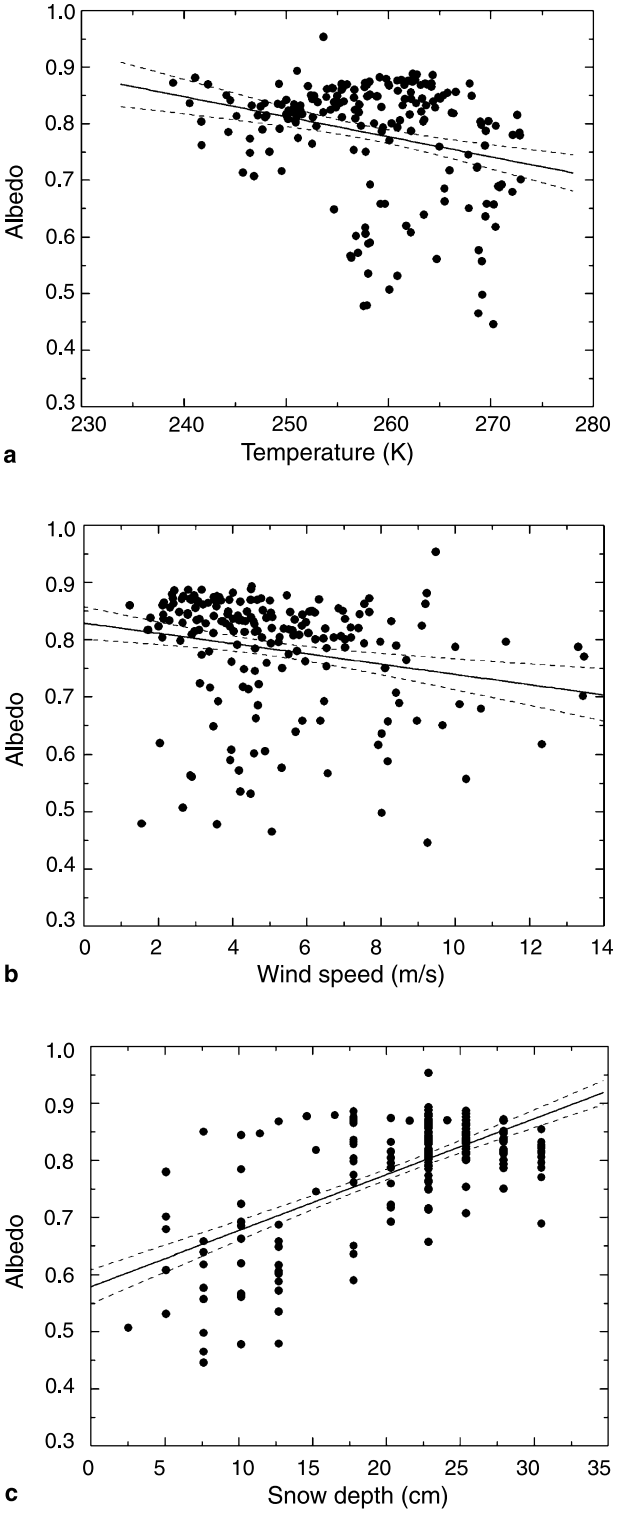

Fig. 8. Scatter plots of daily mean observed snow albedo vs. (**a**) temperature, (**b**) wind speed, and (**c**) snow depth for 2001 and 2002. Data base on 1-minute data for albedo and temperature, 2-minute data for wind and daily values for snow depth from February to snowmelt and from onset of the snow season to mid-November. Linear fit and its significance at the 95% confidence level are superimposed

According to the Bouguer-Lambert-Beer law incoming shortwave radiation entering the snow is exponentially reduced. The remaining intensity at a depth z depends on the initial intensity, the extinction coefficient and depth z. For an extinction coefficient of 7×10^{-4} m, for instance, the radiation measured at 0.1 m and 0.5 m depth amounts 50% and 3% of the incoming radiation at the snowpack surface (Herrmann and Kuhn 1990). The upward reflected radiation is also exponentially absorbed and can be scattered. Thus, the outgoing radiation is a mixed signal of reflectance from various depths, i.e., the integrated outcome of the processes occurring within the snow. Note that in general, the extinction coefficient has even wider range of variability than snow albedo. Unfortunately, no extinction-coefficient measurements and no radiation measurements within the snow were made. For all these reasons both a linear and exponential correlation are examined. Snow albedo increases with increasing snow depth with a correlation of 0.653. An exponential fit provides a similar goodness of fit than the linear fit, for which the former is not considered any further.

Correlation between wind speed and snow albedo is -0.210, i.e., snow albedo decreases with increasing wind speed. The ice-crystal area that reflects shortwave radiation is reduced when the wind destroys ice-crystal structures. The wind can also decrease the snow depth and therefore reduce snow albedo as more radiation from the ground is reflected. The increased wind also may expose long grass/herbs thereby reducing the albedo. Under calm conditions, albedo can increase again by ice crystals that form on obstacles sticking out of the snow and/or trace precipitation (cumulative snow <1 mm) (e.g., Julian days 61–64, Figs. 3, 6; 74–81, Figs. 4, 7).

The correlation between snow age and snow albedo is 0.123, i.e., albedo increases as snow ages. This result is contrary to the expectations, but may be an artifact of the extreme light conditions at Barrow. Note that the sun elevation and length of daylight increase rapidly as time progresses towards spring, and that the correlation coefficient will switch its sign if the negative value of the standard deviation of the correlation coefficient is added. The low correlation factor is also caused by the unequal frequency of the various snow ages. At Barrow, there are many snow-albedo values for relatively new snow, while there are fewer values for aged snow. On average, snowfall occurs every two days (e.g., Figs. 3 and 4). The longest period without snowfall is 15 days in our dataset. Probably, snow age affects snow albedo, but the influence of temperature, wind speed, and snow depth are dominant. The unknown exact time of onset and end of snowfall may play a role why the dataset does not really permit considering the effect of aging snow for the non-melting season. Obviously the governing physical processes are related to metamorphism (temperature gradient in the snow, settling, and windbreak) rather than snow age under these conditions. Since the correlation is insignificant and negligible, and based on the results found for snow-age dependent parameterization in this study we conclude that snow age marginally influences the snow albedo at Barrow.

Multiple correlation analysis provides a multiple correlation of 0.672 between snow albedo, temperature, and snow depth. Inclusion of wind speed increased the multiple-correlation factor to 0.700 demonstrating the influence of wind speed on snow albedo. The multiple-correlation between snow albedo and temperature, wind speed, snow depth, and snow age is 0.705. In other words, snow age only marginally increased the multiple-correlation factor.

5.2 Parameterization of snow albedo

Based on the evaluation of ISBA and SAST for Barrow, and on the results found for prognostic snow-albedo parameterizations for eight sites by Pedersen and Winther (2005), it is advantageous not to use the snow albedo of the previous time step to predict the new value because of error propagation. Therefore, and because snow age is not a significant parameter for snow albedo, and because for climate modeling purposes a parameterization is advantageous that only relies on variables calculated by the model (e.g., air temperature, snow depth, wind speed), we do not consider snow age in parameterizing snow albedo.

Data analysis shows that if snow depth exceeds 0.15 m, temperature and wind gain importance for snow albedo. Obviously, around this depth, the snowpack becomes thick enough so that the effects of the underlying ground are obliterated. Warren and Wiscombe (1980) give a

value of 0.02, 0.08, and 0.2 m liquid water equivalent for a snowpack with 100, 200, and 400 kg/m^3 snow density being thick enough to be semi-infinite (i.e., at all wavelengths albedo is within 1% of that for an infinitely thick snowpack). In Arctic tundra, snow density typically amounts about 300 kg/m^3 for February to March and increases to about 450 kg/m^3 later in the season (e.g., Sturm and Holmgren 1998). Thus, a 0.15 m snow depth broadly corresponds to a water equivalent of 0.045 m meaning that the snowpack is thick enough to not "see" the ground. By using a multiple linear regression fitting method considering wind and temperature for snowpacks deeper than 0.15 m, and wind, temperature and snow depth else wise, we obtain for snow albedo

$$\alpha = \begin{cases} \max(0.35, 0.79 - 0.0018T_R - 0.0045v) & h_s > 0.15\,\text{m} \\ \max(0.585, 0.616 - 0.001T_R - 0.0076v + 0.01h_s) & 0.0254\,\text{m} < h_s \le 0.15\,\text{m} \\ 0.565 & h_s = 0.0254\,\text{m} \end{cases} \quad (7)$$

where T_R, h_s and v are air temperature (°C) at 2-m height, snow depth (cm), and wind speed (m/s). Note that because snow depth is rounded to the full inch, it cannot fall below 0.0254 m if snow is present. The coefficients concerning temperature are negative indicating that snow albedo decreases as temperature increases, which well agrees with theoretical expectations and other observational evidence (e.g., O'Brien and Munis 1975; Wiscombe and Warren 1980). The high coefficient for snow depth reflects the dominance of the effect of optical depth before the snowpack is thick enough to become effectively semi-infinite. Independent of snow depth the impact of wind speed is higher than that of temperature despite the slightly higher correlation coefficient found between observed temperature and snow albedo. The minimum value ensures reasonable values for extreme conditions of wind and temperature like they may occur at high elevation on glaciers in Antarctica or Greenland.

5.3 Evaluation of the new parameterization

For 2003 the new parameterization results in a strong temporal variation of snow albedo similar to that observed (e.g., Fig. 7). In February, snow albedo is sometimes overestimated. In all months, snow albedo is often underestimated after snowfall events. If snow depth is close to the threshold decisive for inclusion or ignoring snow depth in the snow-albedo calculation, the new parameterization may provide an increase, while a decrease is observed and vice versa (e.g., Figs. 4 and 7 around Julian days 57, 95). Close below this depth, the snowpack's optical depth may sometimes be already thick enough in nature to obliterate the ground signal, but the parameterization still considers the snow depth impact. Consequently, snow albedo is underestimated. Sometimes, however, close above this depth the snowpack may be still too thin to obliterate the ground signal, but the parameterization already ignores the depth impact leading to an overestimation of snow albedo. In 2003, the new parameterization predicts too strong a decay after snow depth falls below 0.1 m (Fig. 7e).

The 2003 RMSE and correlation coefficient amount 0.091 and 0.483, respectively (Fig. 5). The SDE (0.092) indicates low uncertainty caused by observations. Based on the BIAS (0.064), systematic errors are small. Simulated and observed snow albedo differ insignificantly. Based on these results we conclude that ARM data are well suitable for development of snow-albedo parameterization for low-precipitation tundra environments.

5.4 Comparison with previous parameterizations

The new parameterization performs better when the snowpack melts rapidly within a week (2002; Fig. 6e) than slowly over a month (2003; Fig. 7e). Snow albedo is underestimated as snow depth falls below 5 cm. Here the fixed value (0.585) and the uncertainty in snow depth measurements play a role.

Since the 2001 and 2002 data have been used for the development of Eq. (7), the correlation coefficients are higher and RMSE are lower than for 2003 or overall three years (Fig. 5). In contrast to the other parameterizations, the new parameterization provides positive correlations between simulated and observed snow albedo (Fig. 5) and simulated and observed values insignificantly differ (Table 1) for all three years. The new parameterization provides better correlation between simulation and observations than all other

parameterizations for all years (Fig. 5). Like HTSVS and SAST, and in contrast to ECHAM and ISBA simulated and observed values always agree within a factor of 2. The 2003 BIAS of the new parameterization is of similar magnitude than those of the other parameterizations. The 2003 SDE of the new parameterization is about the size as those of the age dependent parameterizations, while ECHAMs SDE is nearly twice as large (Table 1).

6. Conclusions

The feasibility of data obtained radiometrically at the Barrow, Alaska (USA), ARM site for use in the evaluation and development of snow-albedo parameterizations is examined for a low-precipitation tundra environment. Various examples of snow-albedo parameterizations commonly used in NWPMs or GCMs are tested for the snow seasons 2001–2003. Snow albedo derived from the ARM data shows a complex temporal behavior that cannot be captured by a fixed value, which is the approach used in some NWPMs and GCMs.

As evidenced by the BIAS, parameterizations are sensitive to a certain degree to thresholds (e.g., for the temperature regime, snow depth, cumulative snow required for reset/refresh of albedo). Frequent trace precipitation (<1 mm), effects from low snowfall rates and extended periods without snowfall seem to be especially challenging for snow-albedo modeling. The choice of the maximum and minimum snow albedo may cause offsets. As demonstrated by comparison of the ECHAM and ECHAM5 parameterization, the choice of the threshold may improve the correlation, but not necessarily the overall performance.

ECHAM, HTSVS, ISBA and SAST predict less temporal variability in snow albedo than observed. The ECHAM approach, an example of a solely temperature-based parameterization, does not perform well under Arctic conditions because it reaches the maximum albedo (0.9) when temperature falls below $-10\,^{\circ}$C. This is the case most of the time in the snow season at high latitudes. Consequently, this parameterization overestimates the snow albedo, and fails to capture the temporal pattern; simulated and observed snow albedo differ by a factor of 2 more than 2% of the time.

The snow-albedo parameterization of HTSVS, which is an example of a snow-age dependent parameterization, simulates a too rapid decrease in snow albedo compared to the observations. In general, it underestimates the snow albedo because maximum snow albedo is assumed too low. It provides better results for the melting period compared to the cold period.

The formulations used in SAST and ISBA belong to the prognostic snow-albedo parameterizations. Their main shortcoming is that an initially incorrect snow albedo value will propagate the error. During periods of frequent snow events or strong snowfall, a too high maximum value (e.g., 0.92 as used in SAST) leads to overestimates, while a maximum value of 0.85 as used in ISBA leads to a better agreement with observations. Both parameterizations predict a too rapid decrease of snow albedo, and hence underestimate snow albedo in periods without snowfall. During snowmelt the parameterizations considering snow age (HTSVS, SAST, and ISBA) perform better than the temperature dependent (ECHAM, ECHAM5) parameterizations.

Analysis of the meteorological and radiation data collected at Barrow during 2001–2002 shows that snow albedo decreased with increasing temperature and with increasing wind speed for snow depth greater than 0.15 m, while below this depth it also decreased with decreasing snow depth. Temperature, wind and snow depth are significant parameters for modeling snow albedo at Barrow, while the influence of the snow age is insignificant. A new snow-albedo parameterization based on these findings considers air temperature, snow depth, and wind speed for snow less than 0.15 m depth, and air temperature and wind speed only above that threshold. Data from 2003 serve for the evaluation of the parameterization and comparison with the performance of the other parameterization evaluated here. The developed snow-albedo parameterization performs better than the other snow-albedo parameterizations evaluated. These findings demonstrate that the Barrow ARM data stream is well suited for model development and evaluation purposes, and fulfills the criteria to be achieved for climate evaluation purposes as they are lined out by Goody et al. (2002).

Future work on snow-albedo parameterizations requires the step from offline evaluation, where

the parameterizations are driven by observations, to evaluation in a coupled mode, where the parameterizations are driven by simulated forcing from a NWPM or GCM. Such evaluation needs inclusion of spatial variability and vegetative masking effects by use of remote sensing data in addition to ground based evaluation. It must include assessment of the interaction between the snow-albedo parameterization and the driving model to elaborate whether failings are due to the forcing or parameterization or the interplay of the parameterization and driving model.

Acknowledgements

We thank D. Truffer-Moudra and the anonymous reviewers for fruitful discussion. This research was supported by DOE grant DEFG0394ER747 from the Atmospheric Radiation Measurement program, NASA, and NSF under contracts NNG04GF35G, and OPP0327664.

References

Abdalati W, Steffen K (1997) Snowmelt on the Greenland ice sheet as derived from passive microwave satellite data. J Climate 10: 165–75

Alaska Climate Research Center (2004) *http://climate.gi.alaska.edu/*

Anthes RA, Kuo YH, Hsie EY, Low-Nam S, Bettge TW (1989) Estimation of skill and uncertainty in regional numerical models. Quart J Roy Meteorol Soc 111: 763–806

Baker DG, Ruschy DL, Wall DB (1990) The albedo decay of prairie snow. J Appl Meteor 29: 179–87

Baker JM, Davis KJ, Liknes GC (1999) Surface energy balance and boundary layer development during snowmelt. J Geophys Res 104D: 19611–21

Bohren CF, Barkstrom RB (1974) Theory of the optical properties of snow. J Geophys Res 79: 4527–35

Bonan, GB, Oleson KW, Vertenstein M, Levis S, Zeng X, Dai Y, Dickinson RE, Yang Z-L (2002) The land surface climatology of the community land model coupled to the NCAR community climate model. J Climate 15: 1115–30

Boone A (2002) Description du schema de neige ISBA-ES (Description of the ISBA-ES snow scheme), Note de Centre (technical note), GMME/CNRM/Météo-France, Vol. 70, 53 pp

Boone A, Etchevers P (2001) An intercomparison of three snow schemes of varying complexity coupled to the same land-surface model: local scale evaluation at an Alpine site. J Hydrometeor 2: 374–94

Brun E, Martin E, Simon V, Gendre C, Coleou C (1989) An energy and mass model of snow cover suitable for operational avalanche forecasting. J Glaciol 35: 333–42

Brun E, David P, Sudul M, Brunot G (1992) A numerical model to simulate snow-cover stratigraphy for operational avalanche forecasting. J Glaciol 38: 13–22

Cahill CF (2003) Asian aerosol transport to Alaska during ACE-Asia J Geophys Res 108D: 8664 (DOI: 10.1029/2002JD003271)

Cline DW (1997) Effect of seasonality of snow accumulation and melt on snow surface energy exchanges at a continental alpine site. J Appl Meteor 36: 32–51

Curry JA, Schramm JL, Ebert EE (1993) Impact of clouds on the surface radiation balance of the Arctic Ocean. Meteorol Atmos Phys 51: 197–217

Curry JA, Rossow WB, Randall D, Schramm JL (1996) Overview of Arctic cloud and radiation characteristics. J Climate 9: 1731–64

Dai Y, Zeng X, Dickinson RE (2001) Common land model (CLM) available online at *http://climate.eas.gatech.edu/dai/clmdoc.pdf*

Dai Y, Zeng X, Dickinson RE, Backer I, Bonan GB, Bosilovich MG, Denning AS, Dirmeyer PA, Houser PR, Niu G, Oleson KW, Schlosser CA, Yang ZL (2003) The common land model. Bull Am Met Soc 84: 1013–23

Desborough CE, Pitman AJ (1998) The BASE land surface model. Global Planet Change 19: 3–18

Dethloff K, Rinke A, Lehmann R, Christensen JH, Botzet M, Machenhauer B (1996) A regional climate model of the arctic atmosphere. J Geophys Res 106: 15345–55

Dingman SL (1994) Physical hydrology. Macmillan, New York, 575 pp

Dominé F, Cabanes A, Legagneux L (2002) Structure, microphysics, and surface area of the Arctic snowpack near Alert during ALERT 2000 campaign. Atmos Environ 36: 2753–65

Douville H, Royer JF, Mahfouf JF (1995) A new snow parameterization for the Météo-France climate model. Part I: Validation in stand-alone experiments. Clim Dyn 12: 21–35

Dunkle RV, Bevans JT (1956) An approximate analysis of the solar reflectance and transmittance of a snow cover. J Meteor 13: 212–16

Durand Y, Brun E, Merindol L, Guyomarch G, Lesaffre B, Martin E (1993) A meteorological estimation of relevant parameters for snow models. Ann Glaciol 18: 65–71

Ek MB, Mitchell KE, Lin Y, Rogers E, Grunmann P, Koren V, Gayno G, Tarpley JD (2003) Implementation of Noah land surface model advances in the National Centers for Environmental Prediction operational mesoscale Eta model. J Geophys Res 108(D22): 8851 (DOI: 10.1029/2002JD003296)

Ellingson RG, Stamnes K, Curry JA, Walsh JE, Zak BD (1999) Overview of North Slope of Alaska/adjacent Arctic Ocean science issues. J Climate 12: 46–63

Essery R, Etchevers P (2004) Parameter sensitivity in simulations of snowmelt. J Geophys Res 109: D20111 (DOI: 10.1029/2004JD005036)

Essery R, Yang Z (2001) An overview of models participating in the Snow Model Intercomparison Project (SnowMIP), SnowMIP Workshop, 11 July 2001, 8th Scientific Assembly of IAMAS Innsbruck, see *http://www.cnrm.meteo.fr/snowmip/*

Essery R, Martin E, Douville H, Fernández A, Brun E (1999) A comparison of four snow models using observations from an alpine site. Climate Dyn 15: 583–93

Essery RLH, Blyth EM, Harding RJ, Lloyd CM (2005) Modelling albedo and distributed snowmelt across a low hill on Svalbard. Nordic Hydrol 36: 207–18

Etchevers P, Martin E, Brown R, Fierz C, Lejeune Y, Bazile E, Boone A, Dai Y-J, Essery R, Fernandez A, Gusev Y, Jordan R, Koren V, Kowalczyk E, Nasonova NO, Pyles RD, Schlosser A, Shmakin AB, Smirnova TG, Strasser U, Verseghy D, Yamazaki T, Yang Z-L (2004) Validation of the surface energy budget simulated by several snow models. Ann Glaciol 38: 150–8

Fernandez A (1998) An energy balance model of seasonal snow evolution. Phys Chem Earth 23: 661–6

Flerchinger GN, Baker JM, Spaans EJA (1996) A test of the radiative energy balance of the SHAW model for snow-cover. Hydrol Process 10: 1359–67

Friedrich K, Mölders N (2000) On the influence of surface heterogeneity on latent heat-fluxes and stratus properties. Atmos Res 54: 59–85

Fröhlich K, Mölders N (2002) Investigations on the impact of explicitly predicted snow metamorphism on the micro-climate simulated by a meso-β/γ-scale non-hydrostatic model. Atmos Res 62: 71–109

Goody R, Anderson J, Karl T, Miller RB, North G, Simpson J, Stephens G, Washington W (2002) Why monitor the climate? Bull Am Meteor Soc 83: 873–8

Gray DM, Landine PG (1987) Albedo model for shallow prairie snow covers. Can J Earth Sci 24: 1760–68

Hansen J, Russell G, Rind D, Stone P, Lacis A, Lebedeff S, Ruedy R, Travis L (1983) Efficient three-dimensional global models for climate studies: model I and II. Mon Wea Rev 111: 609–62

Herrmann A, Kuhn M (1990) Schnee und Eis. In: Baumgartner A, Liebscher H-J (eds) Allgemeine Hydrologie – quantitative Hydrologie, Lehrbuch der Hydrologie, Band 1, Gebrüder Borntraeger, Würzburg, pp. 271–312

Jacobson MZ (1999) Fundamentals of atmospheric modeling. Cambridge University Press, New York, 656 pp

Jordan R (1991) A one-dimensional temperature model for a snow cover. Technical documentation for SNTHERM 89. US Army Corps of Engineers, CRREL Special Report, 61 pp

Kondo J, Yamazaki T (1990) A prediction model for snowmelt, snow-surface temperature and freezing depth using a heat balance method. J Appl Meteorol 29: 375–84

Kramm G, Beier N, Foken T, Müller H, Schröder P, Seiler W (1996) A SVAT scheme for NO, NO_2, and O_3 – model description. Meteorol Atmos Phys 61: 89–106

Kreyszig E (1970) Statistische Methoden und ihre Anwendung. Vanden Hoeck & Ruprecht, Göttingen, 422 pp

Legagneux L, Taillandier A-S, Dominé F (2004) Grain growth theories and the isothermal evolution of the specific surface area of snow. J Appl Phys 95: 6175–84

Lehning M, Bartelt P, Brown R, Russi T, Stöckli U, Stucki T, Zimmerli M (1998) A new network of automatic weather and snow stations and supplementary model calculations providing high resolution snowpack information to the avalanche warning services in Switzerland. In: Proc. Int. Snow Science Workshop, September 27 to October 1, 1998, Sunriver, Oregon, USA

Leung LR, Ghan SJ (1995) A subgrid parameterization of orographic precipitation. Theor Appl Climatol 52: 95–118

Liljequist GH (1956) Energy exchange of an Antarctic snowfield. Short-wave radiation (Maudheim, 71°03′S, 10°56′W). Norwegian-British-Swedish Antarctic Expedition, 1949–52, Scientific results, Vol. 2, Pt 1A, Oslo, Norsk, Polarinstitutt, 107 pp

Liston GE (2004) Modelling regional and global scale subgrid heterogeneous snow cover. J Climate 17: 1381–97

Liston GE, Sturm M (1995) A snow-transport model for complex terrain. J Glaciol 44: 498–516

Liu J, Zhang Z, Inoue J, Horton RM (2007) Evaluation of snow/ice albedo parameterization and the impacts on sea ice simulations. Int J Climatol 27: 81–91

Loth B, Graf HF (1998) Modeling the snow cover in climate studies 2. The sensitivity to internal snow parameters and interface processes. J Geophys Res 103: 11329–40

Lynch AH, Chapman WL, Walsh JE, Weller G (1995) Development of a regional climate model of the western Arctic. J Climate 8: 1555–70

Mabuchi K, Sato Y, Kida H, Saigusa N, Oikawa T (1997) A biosphere-atmosphere interaction model (BAIM) and its primary verifications using grassland data. Pap Meteorol Geophys 47: 115–40

Manabe S (1969) Climate and the ocean circulation – 1. The atmospheric circulation and the hydrology of the Earth's surface. Mon Wea Rev 97: 739–74

Matthews E (1983) Global vegetation and land use: New high-resolution data bases for climate studies. J Appl Meteor 22: 474–87

Meyer SL (1975) Data analysis for scientists and engineers. Wiley, New York London Sydney Toronto, 513 pp

Mölders N, Raabe A, Tetzlaff G (1996) A comparison of two strategies on land surface heterogeneity used in a mesoscale β-meteorological model. Tellus 48A: 733–49

Mölders N, Haferkorn U, Döring J, Kramm G (2003) Long-term investigations on the water budget quantities predicted by the hydro-thermodynamic soil vegetation scheme (HTSVS) – Part I: Description of the model and impact of long-wave radiation, roots, snow, and soil frost. Meteorol Atmos Phys 84: 115–35

Mölders N, Jankov M, Kramm G (2005) Application of Gaussian error propagation principles for theoretical assessment of model uncertainty in simulated soil processes caused by thermal and hydraulic parameters. J Hydrometeorol 6: 1045–62

O'Brien HW, Munis RH (1975) Red and near-infrared spectral reflectance of snow. In: Rango A (ed) Applications of satellite snow cover observations, NASA SP-391, Washington, DC, pp. 345–60

Oke TR (1978) Boundary layer climates. Routledge, London New York, 435 pp

Pederson CA, Winther J-G (2005) Intercomparison and validation of snow-albedo parameterization schemes in climate models. Clim Dyn 25: 351–62 (DOI: 10.1007/s00382-005-0037-0)

Pielke RA (2002) Mesoscale meteorological modeling. Academic Press, New York, 676 pp

Plüss C, Ohmura A (1997) Longwave radiation on snow-covered mountainous surfaces. J Appl Meteor 36: 818–24

Robinson DA, Kukla G (1985) Maximum surface albedo of seasonally snow-covered lands in the Northern Hemisphere. J Appl Meteor 24: 402–11

Robinson DA, Dewey KF, Heim RR Jr (1993) Global snow cover monitoring: an update. Bull Amer Meteor Soc 74: 1689–96

Roeckner E, Arpe K, Bengtsson L, Christoph M, Claussen M, Dümenil L, Esch M, Giorgetta M, Schlese U, Schulzweida U (1996) The atmospheric circulation model ECHAM-4: Model description and simulation of present-day climate. Reports of the Max-Planck-Institute, Hamburg, Vol. 218, 90 pp

Roeckner E, Bäuml G, Bonaventura L, Brokopf R, Esch M, Giorgetta M, Hagemann S, Kirchner I, Kornblueh L, Manzini E, Rhodin A, Schlese U, Schulzweida U, Tompkins A (2003) The atmospheric general circulation model ECHAM5 – Part I. Technical report 349, Max Planck Institute for Meteorology, 27 pp

Roesch A, Roeckner E (2006) Assessment of snow cover and surface albedo in the ECHAM5 general circulation model. J Climate 19: 3828–43

Roesch AH, Gilgen M, Wild M, Ohmura A (2001) A new snow cover fraction parametrization for the ECHAM4 GCM. Clim Dyn 17: 933–45

Seth A, Giorgi F, Dickinson RE (1994) Simulating fluxes from heterogeneous land surfaces: explicit subgrid method employing the biosphere-atmosphere transfer scheme (BATS). J Geophys Res 99D: 18651–67

Shaw GE (1991) Aerosol chemical components in Alaska air masses I, aged pollution. J Geophys Res 96: 22357–68

Shmakin A (1998) The updated version of SPONSOR land surface scheme: PILPS-influenced improvements. Global Planet Change 19: 49–62

Slater AG, Schlosser CA, Desborough CE, Pitman AJ, Henderson-Sellers A, Robock A, Ya Vinnikov K, Mitchell K, Boone A, Braden H, Chen F, Cox PM, de Rosnay P, Dickinson RE, Dai Y-J, Duan Q, Entin J, Etchevers P, Gedney N, Ye Gusev M, Habets F, Kim J, Koren V, Kowalczyk E, Nasonova ON, Noilhan J, Schaake J, Shmakin AB, Smirnova TG, Verseghy D, Wetzel P, Xue Y, Yang Z-L, Zeng Q (2001) The representation of snow in land surface schemes: results from PILPS 2(d). J Hydrometeorol 2: 7–25

Stokes GM, Schwartz SE (1994) The atmospheric radiation measurement (ARM) program: programmatic background and design of the cloud and radiation testbed. Bull Amer Meteor Soc 75: 1201–21

Strack JE, Liston GE, Pielke RA (2004) Modeling snow depth for improved simulation of snow-vegetation-atmosphere interactions. J Hydrometeorol 5: 723–34

Sturm M, Holmgren J (1998) Differences in compaction behavior of three climate classes of snow. Ann Glaciol 26: 125–30

Sugiura K, Yang D (2003) Systematic error aspects of gauge-measured solid precipitation in the Arctic, Barrow, Alaska. Geophys Res Lett 4: 1192 (DOI: 10.1029/2002GL015547)

Sun S, Jin J, Xue Y (1999) A simple snow-atmosphere-soil transfer (SAST) model. J Geophys Res 104: 19587

Tao X, Walsh JE, Chapman WL (1996) An assessment of global climate model simulations of Arctic air temperatures. J Climate 9: 1060–76

Tetzlaff G, Dlugi R, Friedrich K, Gross G, Hinneburg D, Pahl U, Zelger M, Mölders N (2002) On modeling dry deposition of long-lived and chemically reactive species over heterogeneous terrain. J Atmos Chem 42: 123–55

US Army Crops of Engineers (1956) Snow hydrology: summary report of the snow investigations, Washington, DC: US Department of Commerce Office of Technical Services PB 151660, 462 pp

Verseghy DL (1991) CLASS – A Canadian land surface scheme for GCMs. I. Soil model. Int J Climatol 11: 111–33

Warren SG, Wiscombe WJ (1980) A model for the spectral albedo of snow. II. Snow containing atmospheric aerosols. J Atmos Sci 37: 2734–45

Wigmosta MS, Lettenmaier DP, Vail LW (1994) A distributed hydrology-vegetation model for complex terrain. Water Res Res 30: 1665–79

Wiscombe WJ, Warren SG (1980) A model for the spectral albedo of snow. I. Pure snow. J Atmos Sci 37: 2712–33

Yamazaki T (1998) A multi-layer heat balance model of snow cover – simulations in Siberia and plans. IHAS 4: 161–8

Yang D, Woo MK (1999) Representativeness of local snow data for large-scale hydrological investigations. Hydrol Process 13: 1977–88

Yang ZL, Dickinson RE, Robock A, Vinnikov KY (1997) Validation of the snow submodel of the biosphere-atmosphere transfer scheme with Russian snow cover and meteorological observational data. J Climate 10: 353–73

Zhou L, Dickinson RE, Tian Y, Zeng X, Dai Y, Yang Z-L, Schaaf CB, Gao F, Jun Y, Strahler A, Myneni RB, Yu H, Wu W, Shaikh M (2003) Comparison of seasonal and spatial variations of albedos from moderate-resolution imaginging sprectroradiometer (MODIS) and common land model. J Geophys Res 108(D15): 4488 (DOI: 10.1029/2002JD003326)